BIOMOLECULES & THERAPEUTICS

Original Article
Biomol Ther 28(5), 389-396 (2020)

Epigenetically Upregulated T-Type Calcium Channels Contribute to Abnormal Proliferation of Embryonic Neural Progenitor Cells Exposed to Valproic Acid

Ji-Woon Kim[1], Hyun Ah Oh[1], Sung Rae Kim[2], Mee Jung Ko[1], Hana Seung[1], Sung Hoon Lee[2,*] and Chan Young Shin[1,*]

[1]Departments of Pharmacology and Advanced Translational Medicine, School of Medicine, Konkuk University, Seoul 05029, [2]College of Pharmacy, Chung-Ang University, Seoul 06974, Republic of Korea

Abstract

Valproic acid is a clinically used mood stabilizer and antiepileptic drug. Valproic acid has been suggested as a teratogen associated with the manifestation of neurodevelopmental disorders, such as fetal valproate syndrome and autism spectrum disorders, when taken during specific time window of pregnancy. Previous studies proposed that prenatal exposure to valproic acid induces abnormal proliferation and differentiation of neural progenitor cells, presumably by inhibiting histone deacetylase and releasing the condensed chromatin structure. Here, we found valproic acid up-regulates the transcription of T-type calcium channels by inhibiting histone deacetylase in neural progenitor cells. The pharmacological blockade of T-type calcium channels prevented the increased proliferation of neural progenitor cells induced by valproic acid. Differentiated neural cells from neural progenitor cells treated with valproic acid displayed increased levels of calcium influx in response to potassium chloride-induced depolarization. These results suggest that prenatal exposure to valproic acid up-regulates T-type calcium channels, which may contribute to increased proliferation of neural progenitor cells by inducing an abnormal calcium response and underlie the pathogenesis of neurodevelopmental disorders.

Key Words: Valproic acid, Embryonic cortical brain, Neural progenitor cells, Epigenetic regulation, Proliferation, T-type calcium channels

INTRODUCTION

Neurodevelopmental disorders can be caused by exposure to environmental toxicants resulting in abnormal neuronal proliferation and/or differentiation. Valproic acid (VPA) is a clinically used mood stabilizer and antiepileptic drug. VPA has been suggested as a teratogen that can induce neurodevelopmental disorders, such as fetal valproate syndrome and autism spectrum disorders (Dalens *et al*., 1980; DiLiberti *et al*., 1984; Williams *et al*., 2001; Ornoy, 2009). VPA induces transcriptional activation by inhibiting histone deacetylase and releasing the condensed chromatin structure (Gottlicher *et al*., 2001). Prenatal exposure to VPA causes dysregulation of genetic transcription, which results in enhanced glutamatergic and abnormal cholinergic neuronal development and behavioral impairments, including social deficits, repetitive behaviors, hyperactivity, cognition deficits, and seizure susceptibility, in VPA rodent models (Kim *et al*., 2014a, 2014b, 2017, 2019). VPA also facilitates the proliferation of neural progenitor cells (NPCs), which might be the cause for the induction of anatomical changes, such as macrocephaly, observed in human patients and animal models exposed to VPA during the embryonic period (Kozma, 2001; Go *et al*., 2012).

The T-type calcium channel is a low-voltage activated channel that regulates calcium-dependent physiological processes at the resting membrane potential in excitable cells or non-excitable cells, such as embryonic progenitor cells (NPCs) (Iftinca and Zamponi, 2009; Louhivuori *et al*., 2013). T-type calcium channels consist of three subtypes—CaV3.1, CaV3.2, and CaV3.3—encoded by the genes *CACNA1G*, *CACNA1H*, and *CACNA1I*, respectively. T-type calcium channels mediate different actions depending on their subtype and the type of

Open Access **https://doi.org/10.4062/biomolther.2020.027**

Received Feb 20, 2020 **Revised** Mar 19, 2020 **Accepted** Mar 25, 2020
Published Online Apr 22, 2020

***Corresponding Authors**
E-mail: sunghoonlee@cau.ac.kr (Lee SH), chanyshin@kku.ac.kr (Shin CY)
Tel: +82-2-820-5675 (Lee SH), +82-2-2030-7834 (Shin CY)
Fax: +82-2-816-7338 (Lee SH), +82-2-2049-6192 (Shin CY)

cell containing the channels (Iftinca and Zamponi, 2009). T-type calcium channels have been implicated in regulating cellular viability, proliferation, and differentiation (Panner *et al*., 2005; Oguri *et al*., 2010; Rodriguez-Gomez *et al*., 2012; Kim *et al*., 2018). We previously showed that the pharmacological blockade of T-type calcium channels severely affects the viability of NPCs but not that of differentiated neural cells, suggesting a critical role of T-type calcium channels in the embryonic developmental period. Consistent with this view, CaV3.1 is expressed during the embryonic period and has decreased expression in the perinatal period (Kim *et al*., 2018). Recent genetic studies implicated CaV3.1 and 3.2 as potential risk genes for neural developmental disorders, such as autism spectrum disorders (Splawski *et al*., 2006; Strom *et al*., 2010) and epilepsy (Chen *et al*., 2003; Singh *et al*., 2007). However, how an abnormality in T-type calcium channels mediates the neuropathophysiological process is unclear.

In this study, we investigated whether genes encoding T-type calcium channels are epigenetic targets during prenatal exposure to VPA and assessed the role of T-type calcium channels in VPA-induced neurodevelopmental abnormalities. We found that the mRNA levels of T-type calcium channels were increased by VPA treatment. CaV3.1 was identified as the epigenetic target of VPA, as its increase was not detected in NPCs treated with valpromide, a carboxamide derivative of VPA that does not inhibit histone deacetylase. The proliferation of VPA was increased in NPCs, and pharmacological blockade of T-type calcium channels prevented this increased proliferation. Cells that differentiated from NPCs treated with VPA exhibited abnormal calcium ion (Ca^{2+}) response to KCl-induced depolarization stimulation. Our results provide a clue for understanding the role of T-type calcium channels in the pathophysiology of neurodevelopmental disorders.

MATERIALS AND METHODS

Animals

Pregnant female Sprague-Dawley rats were obtained from Orient Bio (Gyeonggi-do, Korea). Animal housing and treatments, including anesthesia, euthanasia, and administration of VPA, were carried out in accordance with the principles of laboratory animal care (NIH Publication No. 85-23, revised 1985) and were approved by the animal care and use committee of Konkuk University, Korea (KU14143).

Prenatal exposure to VPA and preparation of cortices

VPA was administered as previously reported (Kim *et al*., 2011). VPA (400 mg/kg) was subcutaneously injected into pregnant Sprague-Dawley rats on embryonic day 12.5 (E12.5). Cortices were collected from embryos on E14.5 and stored at –80°C for further analysis.

Primary culture of cortical NPCs and treatment

Primary NPCs were isolated from the E14.5 cortices obtained from the rat embryos and were maintained in a humidified chamber at 37°C with growth factors, as described previously (Go *et al*., 2012). For differentiation, NPCs were subcultured and seeded in plates or coverslips coated with poly-L-ornithine (1 mg/mL; Sigma-Aldrich, St. Louis, MO, USA) and containing DMEM/F12 medium (Invitrogen, Carlsbad, CA, USA) with B27 (Invitrogen) and without growth factors. After 3 h of recovery time, drugs were added to the NPCs, and the NPCs were incubated for 24 h in a humidified chamber.

Polymerase chain reaction (PCR)

Total RNA was extracted from NPCs or cortices using TRIzol reagent (Invitrogen). The RNA was reverse transcribed using a RevertAid Reverse transcriptase kit (K1622; Fermentas, Waltham, MA, USA). For quantitative real-time PCR, cDNA was amplified with custom-made primers using SYBR® Premix Ex Taq II (RR820A; TaKaRa Bio, Shiga, Japan) in an ABI 7500 real-time PCR system (Applied Biosystems, Foster City, CA, USA). Fold-changes in gene expression were quantified using the comparative threshold cycle (Ct) method. The primer sequences were as follows:

Cacna1g (NM_031601): Forward - 5'-CATGCCACCTTTAGGAACTTTG-3', Reverse - 5'-CGGAGGGTGTCCTTCATAATAC-3'

Cacna1h (NM_153814): Forward - 5'-GCCTTCGACGACTTCATCTT, Reverse - 5'-GTGTCACCCAGGTAGCATTT-3'

Cacna1i (NM_020084): Forward - 5'-ACAGGCGATAACTGGAATGG, Reverse - 5'-GTAGAGCGGTGACACAAACT-3'

18s rRNA (Westmark and Malter, 2007): Forward - 5'-CATTAAATCAGTTATGGTTCCTTTGG-3', Reverse - 5'-TCGGCATGTATTAGCTCTAGAATTACC-3'

Western blot analysis

Tissues and cells were lysed with 2× sample buffer (4% w/v sodium dodecyl sulfate [SDS], 20% glycerol, 200 mM dithiothreitol [DTT], 0.1 M Tris-HCl, pH 6.8, and 0.02% bromophenol blue), including protease and phosphatase inhibitors. Protein samples were quantified using a standard bicinchoninic acid (BCA) analysis and an equal amount of total protein was resolved by SDS-PAGE and transferred to nitrocellulose membranes. The membranes were blocked with 1% skim milk and incubated overnight at 4°C with primary antibodies against CACNA1G, (ab134269; Abcam, Cambridge, UK; 1:2,000), β-actin (A2066; Sigma-Aldrich; 1:50,000), Histone H3 (9715S; Cell Signaling Technology, Beverly, MA, USA; 1:2,500), or acetylated Histone H3 (06-599; Millipore, Billerica, MA, USA; 1:2,500). After washing each membrane three times with 0.1% Tris-buffered saline (TBS-Tween), the blots were incubated with the peroxidase-conjugated secondary antibody for 2 h at 20-25°C. After washing the blots with 0.1% TBS-Tween, bands were detected using Amersham enhanced chemiluminescence reagent (GE Healthcare Life Science, Pittsburgh, PA, USA) and visualized using a LAS-3000 imaging system (Fuji Film, Tokyo, Japan). The band intensity was analyzed using the Multi Gauge v3.0 software (Fuji Film).

Chromatin immunoprecipitation

Chromatin immunoprecipitation was performed as previously reported (Kim *et al*., 2014a). To collect *in vitro* samples, 43 μL of 37% formaldehyde was applied to each well of a six-well plate containing 1.6 mL of culture medium and cultivated NPCs, and the plate was incubated for 15 min at 20-25°C temperature. Subsequently, 225 μL of 1 M glycine was added to each well and incubated for an additional 5 min. Cells were collected, centrifuged (2,000 ×g for 5 min at

4°C), and washed twice with cold phosphate-buffered saline (PBS). For *in vivo* sample preparation, embryonic cortices were collected from embryos exposed to saline or VPA and homogenized in PBS. Aliquots (1.6 mL) of the homogenates received 43 μL of 37% formaldehyde and the mixtures were incubated at 20-25°C temperature for 15 min. After incubation, 225 μL of 1 M glycine was added to each mixture, incubated for 5 min, centrifuged (2,000×g for 5 min at 4°C), and washed twice with cold PBS. The collected samples were lysed with immunoprecipitation (IP) buffer comprising 150 mM sodium chloride, 50 mM Tris-HCl (pH 7.5), 5 mM EDTA, 0.5% IGEPAL CA-630, 1.0% Triton X-100, and protease inhibitor cocktail (4693159001; Roche, Basel, Switzerland) on ice and centrifuged (12,000×g for 1 min at 4°C). The supernatant was discarded, and pellets were washed with cold IP buffer. To shear the chromatin, each pellet was resuspended in IP buffer and sonicated on ice. After centrifugation (12,000×g for 10 min at 4°C), supernatants were collected and the samples were incubated with the designated primary antibody for 12 h at 4°C. A mixture containing 20 μL of IP buffer and 20 μL of protein A/G Agarose beads (20421; Pierce, Rockford, IL, USA) was added to each sample, which was then incubation for 45 min at 4°C on a rotating platform. The samples were washed five times with cold IP buffer and the supernatants were removed. In the respective pellets, 100 μL of 10% Chelex 100 resin (1422822; Bio-Rad, Hercules, CA, USA) was added for DNA isolation. The mixtures were boiled for 10 min at 90°C and centrifuged (12,000×g for 1 min at 4°C). Each supernatant was collected and used for PCR. Primers were designed to complement the promoter region using the Primer Quest Design tool (Integrated DNA Technologies, Coralville, IA, USA). The amplified PCR products were resolved in an ethidium bromide-containing agarose gel and visualized using an ultraviolet lamp. The primers sequences were as follows: *Cacna1g*: Forward - 5'-AGCAAACACTCCCAGACCAC-3', Reverse - 5'-AAATCCGACTCTCCACCTGC-3'; and Glyceraldehyde-3-phosphate dehydrogenase (*Gapdh*): Forward - 5'-TCGTCCGTCCTCTCTACTTT-3', Reverse - 5'-AGCTTTCT GGGCCTTCATAC-3'.

Immunocytochemistry

NPCs were plated on coverslips and fixed with 4% paraformaldehyde at 4°C for 15 min. Samples were permeabilized with 0.1% Triton X-100 dissolved in blocking buffer for 15 min and blocked with blocking buffer comprising 1% bovine serum albumin and 3% fetal bovine serum in PBS for 30 min at 20-25°C temperature. Coverslips were incubated overnight at 4°C with primary antibodies. After three washes, the coverslips were incubated with secondary antibodies conjugated with donkey anti-mouse or donkey anti-rabbit IgG for 1 h at 20-25°C temperature. The coverslips were mounted using Vectashield (Vector Laboratories, Burlingame, CA, USA), and cells were imaged using a model Bx61 fluorescence microscope (Olympus, Tokyo, Japan).

Calcium imaging

Calcium imaging was carried out in NPCs plated on coverslips. Tyrode's solution contained 119 mM NaCl, 2.5 mM KCl, 2 mM $CaCl_2$, 2 mM $MgCl_2$, 25 mM HEPES, and 30 mM glucose (pH adjusted to 7.4). To record calcium entry, coverslips were incubated with 5 mM Fluo3-AM (Invitrogen) in Tyrode's solution supplemented with 0.02% Pluronic F-127 (Sigma-Aldrich) for 30 min at 37°C in the dark. The coverslips were placed in a perfusion chamber on a model Ti2 inverted microscope (Nikon, Tokyo, Japan). Calcium was visualized with a filter set with an excitation peak of 480 nm, 490 nm long pass mirror, 500-550 nm emission filter, and manual flip shutter. Images were captured every 1 s using a model DS-Qi2 camera (Nikon). For depolarization, 15 and 50 mM KCl were added to the perfusion chamber. F_{max} and F_{base} denote maximal increase after stimulation and baseline fluorescence, respectively. Fluorescence change (ΔF) was normalized using the following equation: $\Delta F=(F_{max}–F_{base})/F_{base}$. Calcium responsive cells displayed a ΔF after depolarization>3 times the baseline F_{base}.

Cell viability assay

Cell viability was measured using the standard 3-(4,5-dimethylthiazol-2-yl)-2,5-diphenyltetrazolium bromide (MTT) based assay. After 24 h of drug treatment, MTT (Sigma-Aldrich, 200 μg/mL) was added to each well and incubated for 2 h at 37°C. After removing the medium, dimethyl sulfoxide (DMSO) was added to each well to dissolve the formazan crystals formed by viable cells. Absorbance was measured using a microplate reader at a wavelength of 570 nm and a reference filter of 620 nm, using a SpectrMax190 device (Molecular Devices, Sunnyvale, CA, USA).

Statistical analyses

Statistical analyses were performed using Prism software (GraphPad, La Jolla, CA, USA). Data are presented as mean ± SEM. After confirming the normality of data in datasets, Student's *t*-test, one-way ANOVA, or Kruskal-Wallis test was performed, depending on the study design and dataset. A *p*-value<0.05 was considered statistically significant.

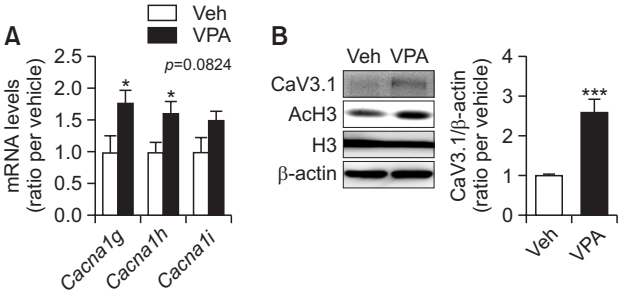

Fig. 1. CaV3.1 mRNA and protein levels are increased in embryonic cortex exposed to VPA. Pregnant rats were exposed to VPA at E12.5, and T-type calcium channel mRNA (*Cacna1g*, *Cacna1h*, and *Cacna1i*) levels and CaV3.1 protein levels were analyzed in the embryo cortex on E14.5. (A) Quantitative real-time PCR results showing mRNA levels of T-type calcium channel subtypes. *Cacna1g* and *Cacna1h* mRNA levels are significantly increased by VPA treatment, and there was an increasing trend in the mRNA level of *Cacna1i* (Veh, n=5, VPA, n=6, *t*-test, *Cacna1g*, $t_{(9)}$=2.441, *p*=0.0373, *Cacna1h*, $t_{(9)}$=2.474, *p*=0.0354, *Cacna1i*, $t_{(9)}$=1954, *p*=0.0824). (B) Blots of CaV3.1, acetylated histone H3, histone H3, and β-actin and quantitative analysis of CaV3.1 protein levels. β-actin was used as the loading control for quantification of the CaV3.1 on blots (N=7 per group, *t*-test, $t_{(12)}$=4.88, *p*=0.0004). Data are presented as mean ± SEM. **p*<0.05 and ****p*<0.001.

RESULTS

Prenatal exposure to VPA increases T-type calcium channels in embryonic cortices

Previously, we showed that VPA induces abnormal genetic transcriptional activation by inhibiting histone deacetylase in the embryonic cortex, which results in neurodevelopmental defects (Kim *et al*., 2014a, 2014b). To investigate whether prenatal exposure to VPA affects transcription of genes for T-type calcium channels in the embryonic cortex, we measured the mRNA levels of *Cacna1g*, *Cacna1h*, and *Cacna1i* in the cortex on E14.5 after exposure to VPA on E12.5. *Cacna1g* and *Cacna1h* were significantly increased, and *Cacna1i* displayed a trend toward an increase, with a *p*-value close to significance (Fig. 1A). Consistent with the increased mRNA levels, CaV3.1 protein levels were also increased by VPA treatment along with increased acetylation in histone H3 (Fig. 1B). These results suggested that *Cacna1g* may be an epigenetic target gene of VPA.

VPA increases T-type calcium channels levels in cultured embryonic NPCs

NPCs are proliferative cells with the potential to differentiate into different types of neuronal cells. In our previous study, we showed that VPA induces abnormal differentiation and proliferation of NPCs, which results in impaired embryonic cortical development (Go *et al*., 2012; Kim *et al*., 2014a, 2014b). Thus, we presently tested whether the VPA-induced increase in CaV3.1 expression also occurs in NPCs. Cultured cortical NPCs were seeded and treated with VPA (0.5 mM) at day *in vitro* (DIV) 0. Twenty-four hours later, we measured *Cacna1g*, *Cacna1h*, and *Cacna1i* mRNA levels using quantitative real-time PCR. Similar to the *in vivo* results, VPA increased *Cacna1g*, *Cacna1h*, and *Cacna1i* mRNA levels (Fig. 2A). To confirm whether these increased mRNA levels induce increased CaV3.1 expression, we measured the levels of CaV3.1 protein by western blotting. Similar to the above mentioned *in vivo* results, VPA increased the levels of CaV3.1 and promoted acetylation in histone H3 in cultured cortical NPCs (Fig. 2B). Consistent with the Western blotting results, immunostaining with CaV3.1 antibodies revealed an increased intensity of CaV3.1 expression in cultured cortical NPCs (Fig. 2C).

VPA up-regulates CaV3.1 expression through epigenetic modulation

To investigate whether VPA promotes CaV3.1 expression through histone modification, we treated NPCs with VPM (0.5 mM), which is a derivative of valproic acid that does not inhibit histone deacetylase. As expected, VPA significantly increased CaV3.1 expression but VPM did not (Fig. 3A). Next, to confirm that the increase in CaV3.1 protein is induced through epigenetic modulation, we treated NPCs with VPA, VPM, and two additional histone deacetylase inhibitors, trichostatin A (0.2 M) and sodium butyrate (0.1 mM). The levels of CaV3.1 were significantly increased by VPA, trichostatin A, and sodium butyrate, but not by VPM (Fig. 3B).

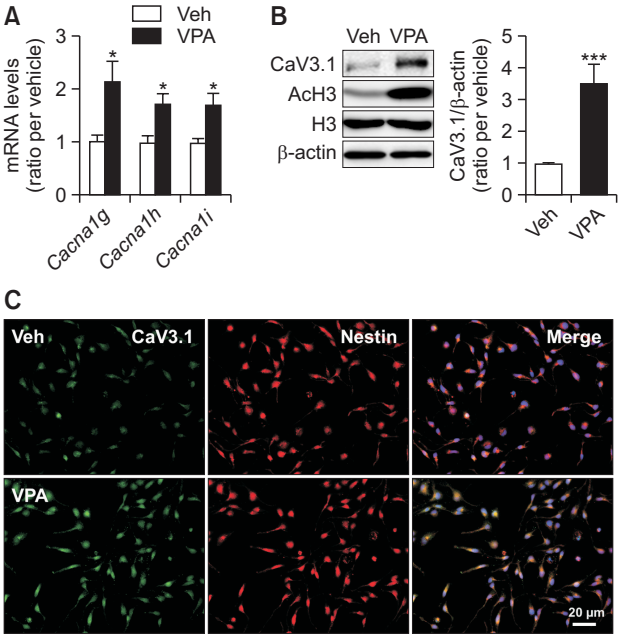

Fig. 2. CaV3.1 mRNA and protein levels are increased in cultured cortical NPCs by VPA treatment. (A) mRNA levels of *Cacna1g*, *1h*, and *1i* were measured through quantitative real-time PCR in the NPCs 24 h after VPA treatment. The mRNA levels of T-type calcium channels were significantly increased by VPA treatment (N=4 per group, *t*-test, *Cacna1g*, $t_{(6)}$=2.822, *p*=0.0303, *Cacna1h*, $t_{(6)}$=3.196, *p*=0.0187, *Cacna1i*, $t_{(6)}$=3.018, *p*=0.0235). (B) Western blots of CaV3.1, acetylated histone H3, histone H3, and β-actin and quantitative analysis of CaV3.1 protein levels. β-actin was used as the loading control for quantification of CaV3.1 on blots (N=6 per group, *t*-test, $t_{(12)}$=4.88, *p*=0.0004). (C) Immunostaining of CaV3.1 in VPA-exposed NPCs at DIV1. Data are presented as mean ± SEM. N=4-6, **p*<0.05 and ****p*<0.001.

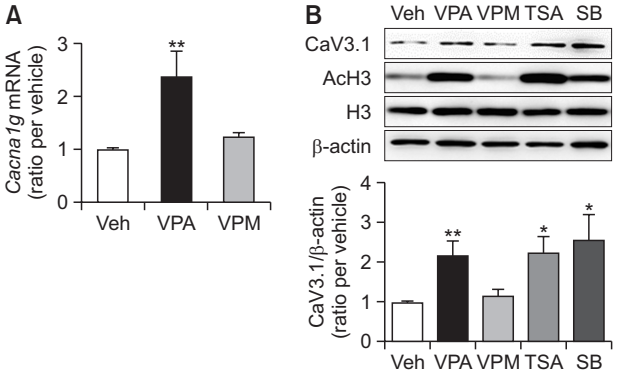

Fig. 3. VPA enhances CaV3.1 expression by inhibiting histone deacetylase. (A) *Cacna1g* mRNA levels analyzed through real-time PCR 24 h after treatment with vehicle, VPA or valpromide in NPCs. Treatment with VPA, but not VPM, increased the levels of *Cacna1g* mRNA, compared to vehicle treatment (N=11 per group, Kruskal-Wallis test followed by Dunn's multiple comparison test, H=7.928, *p*=0.0190). (B) Protein levels of CaV3.1 and acetylated histone H3 in NPCs and quantitative analysis of CaV3.1 protein levels. β-actin was used as a loading control for quantification of the proteins on blots. CaV3.1 protein levels were increased by VPA, TSA, and SB, compared to vehicle treatment (N=4-5, one-way ANOVA followed by *t*-test, $F_{(4, 19)}$=3.374, *p*=0.0302). Data are presented as mean ± SEM. **p*<0.05 and ***p*<0.01.

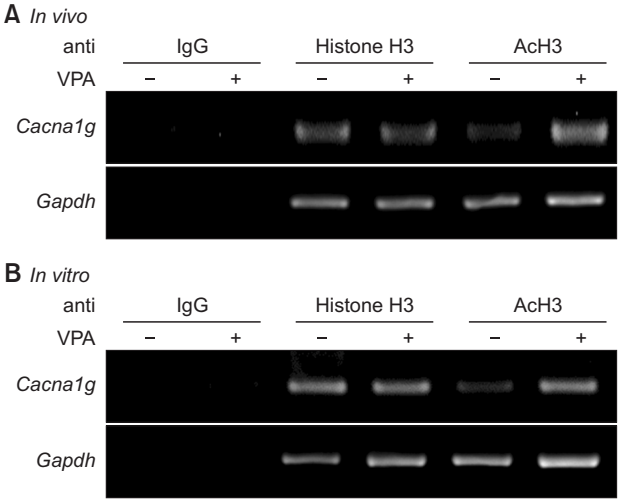

Fig. 4. VPA exposure induces acetylation in histone H3 binding to CaV3.1 promoter region. The chromatin immunoprecipitation assay was performed in the VPA-exposed cortices from E14.5 brains (A) and VPA-treated embryonic cortical NPCs (B). Increased acetylation in histone H3 binding to the promoter region of *Cacna1g* was observed in the embryonic cortex exposed to VPA and VPA-treated NPCs.

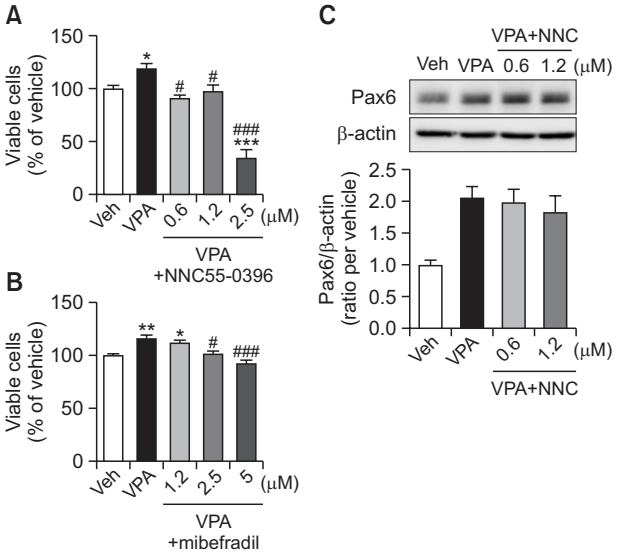

Fig. 5. Pharmacological blockade of T-type calcium channels prevents abnormally increased proliferation in VPA-treated NPCs. (A, B) MTT analysis was conducted 24 h after the pharmacological blockade of calcium channels using (A) NNC55-0396 and (B) mibefradil in VPA-pretreated NPCs. NNC55-0396 and mibefradil treatment prevented an increase in the proliferation of VPA-treated NPCs [(A): N=4-8, one-way ANOVA followed by Tukey's multiple comparison test, $F_{(4, 27)}$=28.7, p<0.0001, (B): N=4, one-way ANOVA followed by Tukey's multiple comparison test, $F_{(4, 15)}$=15.64, p<0.0001]. (C) Levels of Pax6 protein were measured through western blotting 24 h after NNC55-0396 treatment in VPA-pretreated NPCs. NNC55-0396 did not block an increase in Pax6 levels in VPA-treated cells at 0.6 and 1.2 μM (N=3-4, one-way ANOVA followed by Tukey's multiple comparison test, $F_{(3, 11)}$=6.074, p=0.0108). Data are presented as mean ± SEM. N=4-5, *p<0.05, **p<0.01, ***p<0.001 vs. vehicle, $^{\#}p$<0.05, $^{\#\#\#}p$<0.001 vs. VPA-treated group.

VPA promotes acetylation in histone H3 bound to the *Cacna1g* promoter region in embryonic cortices and cortical NPCs

Next, we examined the binding of acetylated histone H3 to promoter regions of the *Cacna1g* gene to confirm that the changed CaV3.1 expression is induced from epigenetic modulation by VPA. We performed chromatin IP with E14.5 cortices from embryos exposed to VPA on E12.5 and cultured cortical NPCs 24 h after VPA treatment. Increased binding of acetylated H3 to the *Cacna1g* promoter region was observed in both embryonic cortices and NPCs (Fig. 4). These results suggested that CaV3.1 is an epigenetic target of VPA.

T-type calcium channels mediate increased proliferation in NPCs exposed to VPA

We previously showed that VPA facilitates proliferation and promotes Pax6 expression in the embryonic cortex and NPCs, which results in macrocephaly and excitatory-inhibitory imbalance, respectively, in an animal model of autism induced by prenatal exposure to VPA (Go *et al*., 2012; Kim *et al*., 2014b). Given that T-type calcium channels are important in regulating cell cycling, proliferation, and differentiation (Panner *et al*., 2005; Lory *et al*., 2006; Oguri *et al*., 2010; Rodriguez-Gomez *et al*., 2012; Louhivuori *et al*., 2013), the increased CaV3.1 expression may mediate increased proliferation or altered differentiation in VPA-treated NPCs. To confirm this hypothesis, we applied T-type calcium channel blockers to VPA-treated NPCs and conducted the MTT assay to investigate the effect on the number of viable cells. The blockers used were NNC55-039, which blocks CaV3.1 and CaV3.2 (Huang *et al*., 2004; Taylor *et al*., 2008) and mibefradil, which is a broad T-type calcium channel blocker and weak L-type calcium channel blocker (Martin *et al*., 2000). VPA treatment increased the number of viable cells compared to vehicle treatment, indicating that proliferation of NPCs was increased by VPA (Fig. 5A, 5B). NNC55-0396 blocked the increased number of viable cells in VPA-treated NPCs at 0.6 and 1.2 μM. However, at the highest concentration of 2.5 μM, NNC55-0396 treatment resulted in a reduction in the number of viable NPCs, compared to vehicle and VPA treatments (Fig. 5A), indicating the induction of cell death by a strong blockade of T-type calcium channels as previously reported (Kim *et al*., 2018). Similarly, mibefradil prevented an increase in the number of viable cells in VPA-treated NPCs over 2.5 μM (Fig. 5B). Next, we measured the levels of Pax6 after treatment with NNC55-0396 in VPA-pretreated NPCs to investigate the role of T-type calcium channels in the facilitated glutamatergic neuronal differentiation by VPA. T-type calcium channel blockade did not alter the increased levels of Pax6 by VPA treatment (Fig. 5C). These results suggested that T-type calcium channels may contribute to the increased proliferation, but not differentiation, of NPCs by VPA.

Differentiated NPCs exposed to VPA have increased activity-dependent calcium influx

Next, we questioned whether activity-dependent calcium influx is altered in differentiated neural cells from VPA-treated NPCs. We measured the calcium response to KCl-induced depolarization stimulation using Fluo3-AM in the differentiated neural cells from NPCs treated with either vehicle or VPA 24 hrs prior. Differentiated neural cells from VPA-treated

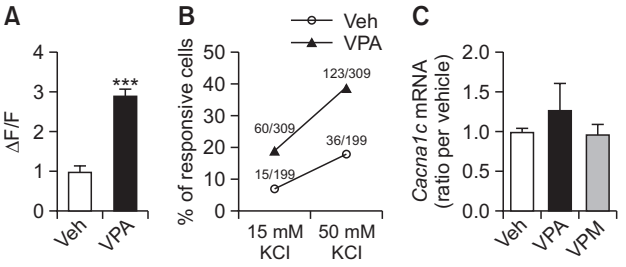

Fig. 6. Differentiated NPCs pretreated with VPA display increased activity-dependent calcium entry. Calcium was measured using Fluo-3AM in NPCs after 15 mM or 50 mM KCl treatment of VPA-pretreated NPCs. (A) The maximum amplitude of calcium responses of NPCs treated with vehicle or VPA to 15 mM KCl. Maximum fluorescence was normalized to baseline (F_{base}). VPA-treated NPCs showed an enhanced Ca^{2+} influx in response to 15 mM KCl stimulation (N=13, *t*-test, $t_{(24)}$=8.55, p<0.0001). (B) The percentage of calcium responsive cells exhibiting significantly increased Ca^{2+} response upon stimulation with 15 or 50 mM KCl. (C) Cacna1c mRNA levels measured through real-time PCR were not significantly changed (N=4, $F_{(2, 9)}$=0.6556, p=0.5423). Data are presented as mean ± SEM. ***p<0.001.

NPCs displayed an increase in calcium influx in response to 15 mM KCl-induced depolarization stimulation, compared to differentiated neural cells from vehicle-treated NPCs (Fig. 6A). Calcium responsive cells, in response to both 15 and 50 mM KCl stimulation, were also increased by VPA treatment (Fig. 6B). To confirm whether the increased activity-dependent Ca^{2+} influx was induced by increased levels of L-type calcium channels, we measured the levels of *Cacna1c* mRNA, which encodes CaV1.2, a subunit of L-type calcium channels. Cacna1c mRNA levels were not changed by either VPA or VPM treatment, suggesting that CaV1.2 is not a target of VPA and may not be the cause for the increased Ca^{2+} influx in response to KCl-induced depolarization stimulation (Fig. 6C).

DISCUSSION

In this study, we found that VPA increases the mRNA levels of all subtypes of T-type calcium channels in primary cultured rat NPCs and embryonic rat cortex. CaV3.1 protein levels were increased by other histone deacetylase inhibitors, but not by VPM, suggesting that CaV3.1 is an epigenetic target of VPA during embryonic cortical development. Pharmacological blockade of T-type calcium channels prevented an increase in VPA-induced proliferation of NPCs. Lastly, we found that activity-dependent Ca^{2+} influx is increased in differentiated neural cells from NPCs previously exposed to VPA. Our results may provide a clue for understanding the role of T-type calcium channels in VPA-induced neurodevelopmental impairments.

We found that T-type calcium channels are upregulated by VPA exposure during the embryonic period. T-type calcium channels have been implicated in neurodevelopmental disorders, such as autism spectrum disorders (Splawski *et al*., 2006; Strom *et al*., 2010) and absence seizure (Chen *et al*., 2003; Singh *et al*., 2007). Interestingly, gain of function mutation in these genes has been found in clinical genetic studies, and the patients with these mutated genes displayed severe motor and cognitive impairments and epilepsy (Khosravani *et al*., 2004, 2005; Chemin *et al*., 2018). Transgenic mice overexpressing *Cacna1g* reportedly showed a spike-wave discharge in the thalamocortical network along with behavioral arrest, which is a typical phenotype associated with absence seizure; however, the mice did not display movement impairments like ataxia or tremor (Ernst *et al*., 2009). Of note, prenatal exposure to VPA also induces autism-like behavioral symptoms and increased seizure susceptibility (Kim *et al*., 2014a, 2014b, 2017, 2019). Thus, these lines of evidence might indicate a role of T-type calcium channels in mediating normal neurodevelopment.

We found that VPA increased the number of viable NPCs, indicating that VPA increased the proliferation of NPCs. Of note, the increased proliferation of NPCs exposed to VPA was prevented by T-type calcium channel blockers, suggesting a crucial role of T-type calcium channels in mediating the abnormal proliferation of NPCs exposed to VPA. Indeed, the importance of T-type calcium channels in regulating the cell cycle and cell proliferation has been reported in proliferating cells, such as cancer cells (Hirooka *et al*., 2002; Panner *et al*., 2005; Oguri *et al*., 2010). Thus, it is reasonable speculation that calcium influx through T-type calcium channels is involved in cell-cycle regulation pathways in NPCs. We previously showed that VPA increases the proliferation of NPCs by inhibiting glycogen synthase kinase 3β (GSK3β) activity and activating β-catenin-dependent signaling (Go *et al*., 2012). Thus, calcium influx through T-type calcium channels may be involved in this signaling pathway. Indeed, we previously showed that pharmacological blockade of T-type calcium channels activates GSK3β and induces apoptotic cell death in NPCs (Kim *et al*., 2018). It is conceivable that Ca^{2+} entry via T-type calcium channels may regulate calcium-dependent kinases and its downstream signaling such as AKT-GSK3β (Cross *et al*., 1995; Yano *et al*., 1998), which mediates the physiological processes such as cell cycle regulation in NPCs (Toth *et al*., 2016). We previously showed that VPA increases proliferation in NPCs, which results in an increase in the number of neurons in the rat embryonic brain and leads to macrocephaly in offspring prenatally exposed to VPA (Go *et al*., 2012). Thus, we may hypothesize a possible role of T-type calcium channels in regulating the neural population in the embryonic brain and inducing macrocephaly. This hypothesis awaits further investigation.

Differentiated neural cells from VPA-treated NPCs showed increased Ca^{2+} influx in response to KCl-induced depolarization, suggesting that prenatal exposure to VPA causes an abnormality in activity-dependent Ca^{2+} entry. Given VPA promotes differentiation into excitatory neurons by upregulating Pax6 levels (Kim *et al*., 2014b), it is plausible that the increased number of cells responsive to KCl stimulation might be due to the facilitated differentiation by VPA. We did not see any changes in mRNA levels of *Cacna1c* in NPCs exposed to VPA, suggesting the expression of CaV1.2 is not a cause for the increased Ca^{2+} response to KCl stimulation in the NPCs. Although we cannot rule out that the up-regulation of the other subunits of L-type calcium channels in NPCs exposed to VPA may be responsible for the increased Ca^{2+} influx in response to KCl stimulation, the increased expression of T-type calcium channels by VPA may also be involved in the abnormally increased Ca^{2+} influx. The abnormal activity-dependent Ca^{2+} response and its related signaling in the pathophysiology of VPA-induced neurodevelopmental disorders would be intrigu-

ing to investigate further.

In conclusion, our study suggests that up-regulation of T-type calcium channels mediates the abnormal proliferation in VPA-exposed NPCs, which might lead to neurodevelopmental disorders. Additionally, abnormal activity-dependent Ca^{2+} entry may also contribute to the pathophysiology of VPA-induced neurodevelopmental disorders. How Ca^{2+} derived from T-type calcium channels is involved in the proliferation of NPCs and how abnormal activity-dependent Ca^{2+} signaling affects the pathophysiology of VPA-induced neurodevelopmental disorders require further investigation.

ACKNOWLEDGMENTS

This research was supported by the Chung-Ang University Research Grants in 2019 and by the Korea Institute of Science and Technology (Grant No. 2E30190-20-060).

REFERENCES

Chemin, J., Siquier-Pernet, K., Nicouleau, M., Barcia, G., Ahmad, A., Medina-Cano, D., Hanein, S., Altin, N., Hubert, L., Bole-Feysot, C., Fourage, C., Nitschke, P., Thevenon, J., Rio, M., Blanc, P., Vidal, C., Bahi-Buisson, N., Desguerre, I., Munnich, A., Lyonnet, S., Boddaert, N., Fassi, E., Shinawi, M., Zimmerman, H., Amiel, J., Faivre, L., Colleaux, L., Lory, P. and Cantagrel, V. (2018) De novo mutation screening in childhood-onset cerebellar atrophy identifies gain-of-function mutations in the CACNA1G calcium channel gene. *Brain* **141**, 1998-2013.

Chen, Y., Lu, J., Pan, H., Zhang, Y., Wu, H., Xu, K., Liu, X., Jiang, Y., Bao, X., Yao, Z., Ding, K., Lo, W. H., Qiang, B., Chan, P., Shen, Y. and Wu, X. (2003) Association between genetic variation of CACNA1H and childhood absence epilepsy. *Ann. Neurol.* **54**, 239-243.

Cross, D. A., Alessi, D. R., Cohen, P., Andjelkovich, M. and Hemmings, B. A. (1995) Inhibition of glycogen synthase kinase-3 by insulin mediated by protein kinase B. *Nature* **378**, 785-789.

Dalens, B., Raynaud, E. J. and Gaulme, J. (1980) Teratogenicity of valproic acid. *J. Pediatr.* **97**, 332-333.

DiLiberti, J. H., Farndon, P. A., Dennis, N. R. and Curry, C. J. (1984) The fetal valproate syndrome. *Am. J. Med. Genet.* **19**, 473-481.

Ernst, W. L., Zhang, Y., Yoo, J. W., Ernst, S. J. and Noebels, J. L. (2009) Genetic enhancement of thalamocortical network activity by elevating alpha 1g-mediated low-voltage-activated calcium current induces pure absence epilepsy. *J. Neurosci.* **29**, 1615-1625.

Go, H. S., Kim, K. C., Choi, C. S., Jeon, S. J., Kwon, K. J., Han, S. H., Lee, J., Cheong, J. H., Ryu, J. H., Kim, C. H., Ko, K. H. and Shin, C. Y. (2012) Prenatal exposure to valproic acid increases the neural progenitor cell pool and induces macrocephaly in rat brain via a mechanism involving the GSK-3beta/beta-catenin pathway. *Neuropharmacology* **63**, 1028-1041.

Gottlicher, M., Minucci, S., Zhu, P., Kramer, O. H., Schimpf, A., Giavara, S., Sleeman, J. P., Lo Coco, F., Nervi, C., Pelicci, P. G. and Heinzel, T. (2001) Valproic acid defines a novel class of HDAC inhibitors inducing differentiation of transformed cells. *EMBO J.* **20**, 6969-6978.

Hirooka, K., Bertolesi, G. E., Kelly, M. E., Denovan-Wright, E. M., Sun, X., Hamid, J., Zamponi, G. W., Juhasz, A. E., Haynes, L. W. and Barnes, S. (2002) T-type calcium channel alpha1G and alpha1H subunits in human retinoblastoma cells and their loss after differentiation. *J. Neurophysiol.* **88**, 196-205.

Huang, L., Keyser, B. M., Tagmose, T. M., Hansen, J. B., Taylor, J. T., Zhuang, H., Zhang, M., Ragsdale, D. S. and Li, M. (2004) NNC 55-0396 [(1S,2S)-2-(2-(N-[(3-benzimidazol-2-yl)propyl]-N-methylamino)ethyl)-6-fluoro-1,2,3,4-tetrahydro-1-isopropyl-2-naphtyl cyclopropanecarboxylate dihydrochloride]: a new selective inhibitor of T-type calcium channels. *J. Pharmacol. Exp. Ther.* **309**, 193-199.

Iftinca, M. C. and Zamponi, G. W. (2009) Regulation of neuronal T-type calcium channels. *Trends Pharmacol. Sci.* **30**, 32-40.

Khosravani, H., Altier, C., Simms, B., Hamming, K. S., Snutch, T. P., Mezeyova, J., McRory, J. E. and Zamponi, G. W. (2004) Gating effects of mutations in the Cav3.2 T-type calcium channel associated with childhood absence epilepsy. *J. Biol. Chem.* **279**, 9681-9684.

Khosravani, H., Bladen, C., Parker, D. B., Snutch, T. P., McRory, J. E. and Zamponi, G. W. (2005) Effects of Cav3.2 channel mutations linked to idiopathic generalized epilepsy. *Ann. Neurol.* **57**, 745-749.

Kim, J. W., Oh, H. A., Lee, S. H., Kim, K. C., Eun, P. H., Ko, M. J., Gonzales, E. L. T., Seung, H., Kim, S., Bahn, G. H. and Shin, C. Y. (2018) T-type calcium channels are required to maintain viability of neural progenitor cells. *Biomol. Ther. (Seoul)* **26**, 439-445.

Kim, J. W., Park, K., Kang, R. J., Gonzales, E. L. T., Kim, D. G., Oh, H. A., Seung, H., Ko, M. J., Kwon, K. J., Kim, K. C., Lee, S. H., Chung, C. and Shin, C. Y. (2019) Pharmacological modulation of AMPA receptor rescues social impairments in animal models of autism. *Neuropsychopharmacology* **44**, 314-323.

Kim, J. W., Seung, H., Kim, K. C., Gonzales, E. L. T., Oh, H. A., Yang, S. M., Ko, M. J., Han, S. H., Banerjee, S. and Shin, C. Y. (2017) Agmatine rescues autistic behaviors in the valproic acid-induced animal model of autism. *Neuropharmacology* **113**, 71-81.

Kim, J. W., Seung, H., Kwon, K. J., Ko, M. J., Lee, E. J., Oh, H. A., Choi, C. S., Kim, K. C., Gonzales, E. L., You, J. S., Choi, D. H., Lee, J., Han, S. H., Yang, S. M., Cheong, J. H., Shin, C. Y. and Bahn, G. H. (2014a) Subchronic treatment of donepezil rescues impaired social, hyperactive, and stereotypic behavior in valproic acid-induced animal model of autism. *PLoS ONE* **9**, e104927.

Kim, K. C., Kim, P., Go, H. S., Choi, C. S., Yang, S. I., Cheong, J. H., Shin, C. Y. and Ko, K. H. (2011) The critical period of valproate exposure to induce autistic symptoms in Sprague-Dawley rats. *Toxicol. Lett.* **201**, 137-142.

Kim, K. C., Lee, D. K., Go, H. S., Kim, P., Choi, C. S., Kim, J. W., Jeon, S. J., Song, M. R. and Shin, C. Y. (2014b) Pax6-dependent cortical glutamatergic neuronal differentiation regulates autism-like behavior in prenatally valproic acid-exposed rat offspring. *Mol. Neurobiol.* **49**, 512-528.

Kozma, C. (2001) Valproic acid embryopathy: report of two siblings with further expansion of the phenotypic abnormalities and a review of the literature. *Am. J. Med. Genet.* **98**, 168-175.

Lory, P., Bidaud, I. and Chemin, J. (2006) T-type calcium channels in differentiation and proliferation. *Cell Calcium* **40**, 135-146.

Louhivuori, L. M., Louhivuori, V., Wigren, H. K., Hakala, E., Jansson, L. C., Nordstrom, T., Castren, M. L. and Akerman, K. E. (2013) Role of low voltage activated calcium channels in neuritogenesis and active migration of embryonic neural progenitor cells. *Stem Cells Dev.* **22**, 1206-1219.

Martin, R. L., Lee, J. H., Cribbs, L. L., Perez-Reyes, E. and Hanck, D. A. (2000) Mibefradil block of cloned T-type calcium channels. *J. Pharmacol. Exp. Ther.* **295**, 302-308.

Oguri, A., Tanaka, T., Iida, H., Meguro, K., Takano, H., Oonuma, H., Nishimura, S., Morita, T., Yamasoba, T., Nagai, R. and Nakajima, T. (2010) Involvement of CaV3.1 T-type calcium channels in cell proliferation in mouse preadipocytes. *Am. J. Physiol. Cell Physiol.* **298**, C1414-C1423.

Ornoy, A. (2009) Valproic acid in pregnancy: how much are we endangering the embryo and fetus? *Reprod. Toxicol.* **28**, 1-10.

Panner, A., Cribbs, L. L., Zainelli, G. M., Origitano, T. C., Singh, S. and Wurster, R. D. (2005) Variation of T-type calcium channel protein expression affects cell division of cultured tumor cells. *Cell Calcium* **37**, 105-119.

Rodriguez-Gomez, J. A., Levitsky, K. L. and Lopez-Barneo, J. (2012) T-type Ca2+ channels in mouse embryonic stem cells: modulation during cell cycle and contribution to self-renewal. *Am. J. Physiol. Cell Physiol.* **302**, C494-C504.

Singh, B., Monteil, A., Bidaud, I., Sugimoto, Y., Suzuki, T., Hamano, S., Oguni, H., Osawa, M., Alonso, M. E., Delgado-Escueta, A. V., Inoue, Y., Yasui-Furukori, N., Kaneko, S., Lory, P. and Yamakawa, K. (2007) Mutational analysis of CACNA1G in idiopathic generalized epilepsy. Mutation in brief #962. Online. *Hum. Mutat.* **28**, 524-525.

Splawski, I., Yoo, D. S., Stotz, S. C., Cherry, A., Clapham, D. E. and Keating, M. T. (2006) CACNA1H mutations in autism spectrum dis-

orders. *J. Biol. Chem.* **281**, 22085-22091.
Strom, S. P., Stone, J. L., Ten Bosch, J. R., Merriman, B., Cantor, R. M., Geschwind, D. H. and Nelson, S. F. (2010) High-density SNP association study of the 17q21 chromosomal region linked to autism identifies CACNA1G as a novel candidate gene. *Mol. Psychiatry* **15**, 996-1005.
Taylor, J. T., Huang, L., Pottle, J. E., Liu, K., Yang, Y., Zeng, X., Keyser, B. M., Agrawal, K. C., Hansen, J. B. and Li, M. (2008) Selective blockade of T-type Ca2+ channels suppresses human breast cancer cell proliferation. *Cancer Lett.* **267**, 116-124.
Toth, A. B., Shum, A. K. and Prakriya, M. (2016) Regulation of neurogenesis by calcium signaling. *Cell Calcium* **59**, 124-134.
Westmark, C. J. and Malter, J. S. (2007) FMRP mediates mGluR5-dependent translation of amyloid precursor protein. *PLoS Biol.* **5**, e52.
Williams, G., King, J., Cunningham, M., Stephan, M., Kerr, B. and Hersh, J. H. (2001) Fetal valproate syndrome and autism: additional evidence of an association. *Dev. Med. Child Neurol.* **43**, 202-206.
Yano, S., Tokumitsu, H. and Soderling, T. R. (1998) Calcium promotes cell survival through CaM-K kinase activation of the protein-kinase-B pathway. *Nature* **396**, 584-587.